35th Annual International Conference of the IEEE EMBS
Osaka, Japan, 3 - 7 July, 2013

Analysis of Reliability Metrics and Quality Enhancement Measures in Current Density Imaging*

F. H. Foomany[1], M. Beheshti[1Ω], K. Magtibay[1], S. Masse[2], W. Foltz[3], E. Sevaptsidis[2], P. Lai[2], D. A. Jaffray[3], S. Krishnan[1], K. Nanthakumar[2], and K. Umapathy[1]
Ryerson University[1], Toronto General Hospital[2], Princess Margaret Hospital[3]

Abstract— **Low frequency current density imaging (LFCDI) is a magnetic resonance imaging (MRI) technique which enables calculation of current pathways within the medium of study. The induced current produces a magnetic flux which presents itself in phase images obtained through MRI scanning. A class of LFCDI challenges arises from the subject rotation requirement, which calls for reliability analysis metrics and specific image registration techniques. In this study these challenges are formulated and in light of proposed discussions, the reliability analysis of calculation of current pathways in a designed phantom and a pig heart is presented. The current passed is measured with less than 5% error for phantom, using CDI method. It is shown that Gauss's law for magnetism can be treated as reliability metric in matching the images in two orientations. For the phantom and pig heart the usefulness of image registration for mitigation of rotation errors is demonstrated. The reliability metric provides a good representation of the degree of correspondence between images in two orientations for phantom and pig heart. In our CDI experiments this metric produced values of 95% and 26%, for phantom, and 88% and 75% for pig heart, for mismatch rotations of 0 and 20 degrees respectively.**

I. Introduction

A. Current Density Imaging (CDI)

An MRI based imaging method that enables measurement of current density inside an object was presented in 1989 by Joy et al and was coined current density imaging (CDI) [1]. This imaging technique allows us to measure the current density non-invasively inside the body of an object. It also facilitates providing a 3D map of current density in points that cannot be reached otherwise without invasive plantation of an electrode that may deform the structure of the object [1]. These properties of CDI make it attractive in the study of biological tissues in the presence of external electrical stimulation.

The CDI method was initially applied to phantoms. Scott et al. (1992) demonstrated that the measured current is matching the injected current by 3D measurement of current density [2]. Scott et al. formulated the relationship between noise in CDI and echo time (1992) [3] which can help us obtain optimum sequence parameters for experiments in terms of SNR. A fast MRI sequence called fast low frequency CDI (FLCDI) was developed by Demonte et al. (2003) allowing us to reduce the pulse duration considerably using fast gradient recalled echo (FGRE) which can speed up the CDI procedure [4]. Later on, CDI was applied to euthanized and live animals. Gamba and Delpy performed CDI on piglet head (1998) by placing electrodes in mouth and top of the head and it was shown that the current pathways in the brain skull, muscle and scalp change considerably from live to post-mortem status [5]. Yoon et al. (2001) applied two electrodes to each side of the chest of euthanized pig. Using CDI it was shown that 80% of current passed through chest wall. The current pattern in the heart was reported to be different in chambers of the heart [6]. Sersa et al. studied the current pathways inside a cancerous tumour in a mouse (1997) showing that no current passes through the dead cells at the center of the tumour [7]. Patriciu et al. studied skin burns under surface electrodes used for monitoring electrical activity or applying shock (2005) and found that there is a correlation between burning patterns and areas of high current density [8]. Demonte et al. (2008) performed electrocardiography (ECG) gated CDI in a live pig, attaching electrodes on the chest of the pig in order to study the effect of Taser on a beating heart [9].

B. Challenges and Requirements of CDI

A major constraint in the application of CDI is that the MRI machine is only able to provide the magnetic flux in one direction (B_0) at a time. Therefore in order to obtain all three main components of the induced magnetic field, the object should be positioned in three perpendicular orientations. This restriction compels us to rotate the subject two times. This rotation is problematic in the case of large subjects due to the MRI bore size and subject deformation. This fact has motivated research to calculate current pathways without such rotations [10-12]. This is however, provable that one orientation of magnetic flux does not give a unique current density [11-12].

When the orientations are not perfectly perpendicular we cannot measure the main three components of magnetic field precisely. Therefore in implementing CDI we should avoid the deformation as much as possible and use the registration techniques to match different orientations.

Use of image registration is not new in the realm of MR imaging, but few works have mentioned this in the area of CDI. These works used registration only for mitigating mis-registration introduced by MRI machine [13-14]. Image registration methods employ different similarity metrics and objective functions, such as mutual information, or correlation between images [15]. The right similarity or error metric, for CDI image registration is an open research question to be addressed. In addition, we will need to define

* We thank CIHR (grant number: 111253) for funding this research.
Ω The first two authors share 1st authorship.

a reliability metric, for evaluation of the quality of CD images before and after registration.

C. Problem Definition and Scope of this Work

A reliability metric based on Gauss's law of magnetism is proposed here and suitability and constraints of this metric in evaluation of degree of match between orientations is analyzed.

We will report the results of CDI experiments on a phantom specifically designed to simulate asymmetry and gaps in organs. The design aims to facilitate analysis of the effect of mismatch and cavities in a real tissue. Then we will present the result of CD imaging of a pig heart and demonstrate how the matching problems as well as problems of gaps manifest themselves in such an experiment on CDI of tissues and how reliability metric could be applied to detect such problems.

II. METHOD

A. Science and Methodology of CDI

Low frequency CDI (LFCDI), as performed here, uses the fact that the phase accumulated in the MRI phase image is proportional to the duration of the current pulse and the magnetic field resulted from the current passing through the object. Once the phase images are obtained from MRI, the magnetic field can be calculated using the following equation [1, 5]:

$$\psi = \gamma \cdot B \cdot T_c \qquad (1)$$

where γ is gyromagnetic ratio, B is the induced magnetic field (parallel to MRI main magnetic field), ψ represents accumulated phase and T_c is total current pulse duration. By applying the Maxwell equation that relates magnetic field and current density as follows one can eventually find the current density:

$$J = i_x\left(\frac{\partial B_z}{\partial y} - \frac{\partial B_y}{\partial z}\right) + i_y\left(\frac{\partial B_x}{\partial z} - \frac{\partial B_z}{\partial x}\right) + i_z\left(\frac{\partial B_y}{\partial x} - \frac{\partial B_x}{\partial y}\right) \qquad (2)$$

J is current density vector, B_x, B_y, and B_z are components of magnetic field and i_x, i_y, and i_z are unit vectors in x,y, and z directions respectively. The MRI phase images should be unwrapped and the derivative of the resulting magnetic fields should be calculated by applying derivative templates in order to obtain the current density [2]. For GE MRI images we used quality guided unwrapping[1] in MATLAB, and for Bruker images we used MRIUTIL[2] software.

Current is passed in two phase cycles (PC) as outlined in [2] in opposite ways, so that by subtracting images from two phase cycles and dividing by two, we see the effect of passed current and not the background magnetic field. In order to remove the background noise in each orientation a mask is generated from magnitude MRI images. These masks will be combined after proper translation and rotation to form a 'combined mask' (among orientations) before final calculation of current density. Since MRI is unable to measure magnetic flux outside the subject, the values of derivatives of the magnetic field on the edges are not reliable and should be eroded. Therefore few outer layers of the resulted J should be discarded through an erosion algorithm [2].

B. Design of Phantom

An acrylic phantom (Figure 1.a) was designed for this study. The phantom had two circular copper electrodes affixed at its top/bottom. Two epoxy filled acrylic bars were added to mimic the cavities in the heart while removing the symmetry. The phantoms were filled with a solution of CuSO4, NaCl and H2O to allow passage of current [2].

C. Image Registration

Various registration techniques are proposed and tested for MRI images in literature [15]. In this study intensity based image registration algorithm implemented in MATLAB image processing toolbox was used [16]. The registration is applied on magnitude images and the translation, rotation and scale matrices obtained through this algorithm are applied on phase images.

Figure 1. (a, left) Designed phantom and (b, right) pig heart used for CDI

D. Validation through Gauss's Law of Magnetism

The Gauss's law of magnetism in differential form is:

$$\nabla . B = 0 \qquad (3)$$

where B is the magnetic field in space. Assuming that B_z in a plane is zero (for example when J has only components parallel to z and perpendicular to the plane) yields that [10]:

$$\frac{\partial B_x}{\partial x} + \frac{\partial B_y}{\partial y} = 0 \qquad (4)$$

This could motivate one to estimate the current from one orientation for example through 2D FFT in special cases [10]. This is not generally possible due to the lack of information in one dimension [11]. While the boundary conditions are needed to solve equations 2 and 4 simultaneously, equations 3 or 4 could be used as validation metrics. Use of these equation for verification has been mentioned by Demonte et al. (2002) [13] but is not detailed. In this study we label a point, reliable if for that point:

$$\frac{\partial B_x}{\partial x} + \frac{\partial B_y}{\partial y} < R_0 \qquad (5)$$

1 Bruce Spottiswoode, Quality Guided Unwrap 2D, http://www.mathworks.com/matlabcentral/fileexchange/22504-2d-phase-unwrapping-algorithms/content/QualityGuidedUnwrap2D.m

2 MRIUtil, http://www.pennstatehershey.org/web/nmrlab/resources/software/mriutil

where we define R_0 threshold. One good way to define such threshold is making it dependent on magnitude of *B* itself by defining:

$$R_0 = k(\overline{|B_x|} + \overline{|B_y|}) \quad (6)$$

$\overline{|B_x|}$ and $\overline{|B_y|}$ are the averages of magnetic field in *x* and *y* direction for all the points in the combined mask. The *k* is a factor that is chosen experimentally (It was set to 10 to give a reliability metric of 95% for the phantom without mismatch rotation). The reliability metric was then defined as:

$$RM = N_A / N_B * 100 \quad (7)$$

where N_A denotes the number of reliable points and N_B the number of points in the combined mask.

E. MRI Experimentation

For phantom and pig heart (Figure 1.b) experiments the spin echo sequence was used with Repetition time (TR) of 700ms. Time of echo (TE) was 100ms for phantom and 50ms for pig heart (to increase signal to noise ratio in latter). Phantom experiments were carried out with a 1.5T GE MRI (at Toronto General Hospital), and pig heart experiments were performed by a 7T Bruker MRI (at STTARR facility). Current calculation in CDI is not affected by the strength of main magnetic field. The number of excitations (NEX) in the reported experiments was 3.

E. Design of Experiments

For the phantom we pass the current between the top and bottom copper plates and we calculate the current through CDI. Subsequently, we rotate one of the images (second orientation) 10 and 20 degrees to demonstrate the effect of mismatch on current calculation. We will report the reliability metric in these cases, and will apply intensity based image registration to alleviate the rotation problem. We will repeat a similar procedure for the pig heart and compare the images and results.

III. RESULTS

Table I reports the results for phantom and pig heart. It is notable that in the case of pig heart, the overall values of current are less than the induced current. Figure 2 demonstrates the images for orientations 1 and 2 as a result of applying both phase cycles. It matches our expectation of perfect passage of perpendicular current in *Z* direction. Current density (*Jz* component) images for the phantom and heart (3 adjacent slices) are depicted in Figures 3 and 4.

Figure 5 demonstrates the magnitude images for the pig heart, with and without registration for 20 degrees artificial rotation. For this experiment the movement artifacts show to be minimal both according to the figure, and according to Table I (rows 5 and 6). The registration shows successful in removing the artificial rotation mismatch. Figure 6 shows how the reliability metric could be helpful in evaluation of mismatch between images. This fact could be observed also, in the right column of Table I. Image registration, when applied, shows success in mitigation of rotation mismatch.

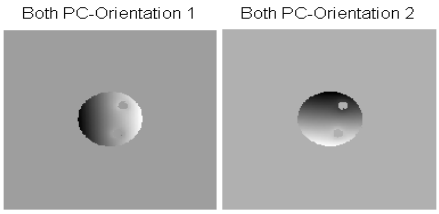

Figure 2. Unwrapped phase images representing current-induced magnetic fields for orientations 1and 2, based on subtraction of phase cycles (PCs)

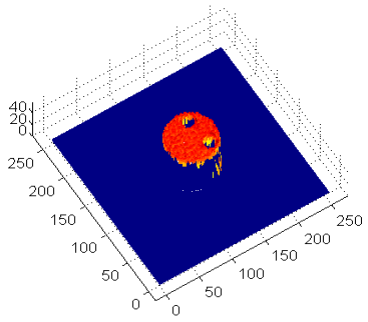

Figure 3. Current density (*Jz)* calculated for phantom (unit:A/m2)

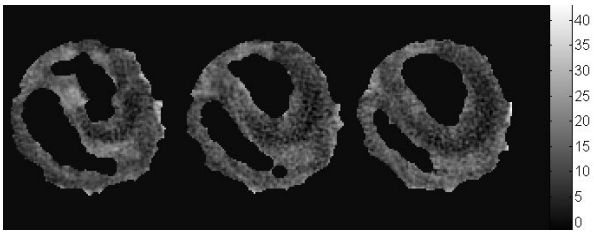

Figure 4. Current density (*Jz*) calcualted for pig heart in 3 adjacent slices 4 millimeter apart (unit:A/m2)

TABLE I. RESULTS OF EXPERIMENTS (ROT:ROTATION ANGLE, REG:REGISTRATION, I: TOTAL CURRENT PASSED, IM:MEASURED CURRENT IN Z DIRECTION THROUGH CDI, EROSION LAYERS WERE 2 FOR PHANTOM AND 4 FOR PIG HEART, SLICE 2)

Subject	**ROT**	**REG**	**I (mA)**	**Im (mA)**	**Reliability Metric**
Phantom	0	N	66.7	63.9	95%
	10'	N	66.7	59.2	56%
	20'	N	66.7	51.4	26%
	20’	Y	66.7	57.4	71%
Pig Heart	0'	N	28.6	18.7	88%
	0'	Y	28.6	18.6	91%
	20'	N	28.6	15.4	75%
	20'	Y	28.6	18.3	90%

IV. DISCUSSION AND CONCLUSION

We reported results of successful CDI experiments of phantom and pig heart. For the phantom the calculated current was closer to the passed current compared to pig

heart. Three causes account for difference in the values of currents in pig heart: 1. components of current are not perpendicular to slices (causing the current densities to be different for 3 slices as shown in Figure 4 for pig heart) 2. Larger perimeter of gaps creates larger eroded current 3. There is mismatch between orientations. We chose a higher value for layers of erosion for pig heart (equal to 4) at the cost of losing currents at the boundaries. While the total current shown in CDI image could be less than passed current, we could comparatively compare the current in various areas. This enables clinical interpretation of results with regard to anatomy of organs in the inner segments especially in studies where the effect is measured for different functional states of the organ.

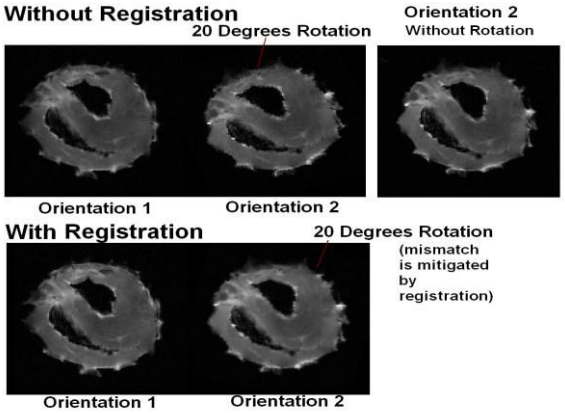

Figure 5. Effect of intensity based image registration. The registration reduces the effect of rotation mismatch. Original mismatch between orientations (without imposed rotation) was minimal for pig heart.

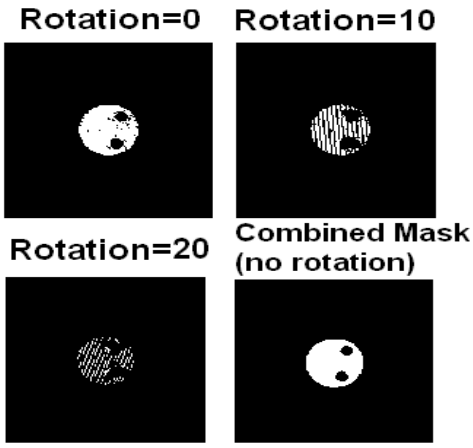

Figure 6. Evaluation of reliability metric in 3 cases: rotation of 0, 10 and 20 degrees. White points represent the reliable points in each case. Combined mask (no rotation) is shown in the bottom right panel for comparison.

The reliability metric proved successful in predicting the imposed mismatch yet its proportionality to the degree of mismatch could be improved. The tested mismatch simulated the post-processing mismatch, and was different from, hypothetically, failing to place the phantom in perpendicular positions in orientations 1 and 2. For example in phantom in that case, the Gauss's law of magnetism would still hold despite the mismatch of masks. Defining a universal threshold for the reliability metric (which renders it proportional to actual mismatch), combining this metric with image registration techniques (as error or similarity metric) as well as extending this work to three dimensions could be pursued in future works.

ACKNOWLEDGMENT

The authors would like to thank Mr. Eugen Hlasny and Mr. Neil Spiller for their valuable comments and help during the MRI data collection. We would also like to thank Mr. James E. Koch, from Ryerson University, for his extensive help in design and implementation of hardware and circuitry.

REFERENCES

[1] M. Joy, G. Scott, and M. Henkelman, "In vivo detection of applied electric currents by magnetic resonance imaging," *Magnetic resonance imaging*, vol. 7, no. 1, pp. 89-94, 1989.

[2] G. Scott, M. Joy, R. Armstrong, and R. Henkelman, "Measurement of nonuniform current density by magnetic resonance," *Medical Imaging, IEEE Transactions on*, vol. 10, no. 3, pp. 362-374, 1991.

[3] G. Scott, M. Joy, R. Armstrong, and R. Henkelman, "Sensitivity of magnetic-resonance current-density imaging," *Journal of Magnetic Resonance*, vol. 97, no. 2, pp. 235-254, 1992.

[4] T. DeMonte, R. Yoon, D. Jorgenson, and M. Joy, "A system for in-vivo cardiac de-fibrillation current density imaging in a pig," in *Engineering in Medicine and Biology Society, 2003. Proceedings of the 25th Annual International Conference of the IEEE*, vol. 1. IEEE, 2003, pp. 175-178.

[5] H. Gamba and D. Delpy, "Measurement of electrical current density distribution within the tissues of the head by magnetic resonance imaging," *Medical and Biological Engineering and Computing*, vol. 36, no. 2, pp. 165-170, 1998.

[6] R. Yoon, T. DeMonte, D. Jorgenson, and M. Joy, "Study of current pathways in porcine heart using current density imaging," *ISMRM, IX'th Sci. Meet. & Exh., Glasgow*, vol. 685, 2001.

[7] I. Sersa, K. Beravs, N. Dodd, S. Zhao, D. Miklavcic, and F. Demsar, "Electric current density imaging of mice tumors," *Magnetic resonance in medicine*, vol. 37, no. 3, pp. 404-409, 1997.

[8] A. Patriciu, K. Yoshida, J. Struijk, T. DeMonte, M. Joy, and H. Stodkilde-Jorgensen, "Current density imaging and electrically induced skin burns under surface electrodes, "*Biomedical Engineering, IEEE Transactions on*, vol. 52, no. 12, pp. 2024-2031, 2005.

[9] T. DeMonte, J. Gao, D. Wang, W. Ma, and M. Joy, "Measurement of current density vectors in a live pig for the study of human electro-muscular incapacitation devices," in *Engineering in Medicine and Biology Society, 2008. EMBS 2008. 30th Annual International Conference of the IEEE*. IEEE, 2008, pp. 5842-5845.

[10] S. Hoon Oh, I. Kon Chun, S. Yeol Lee, M. Hyoung Cho, and C. Woong Mun, "A single current density component imaging by MRCDI without subject rotations," *Magnetic resonance imaging*, vol. 21, no. 9, pp. 1023-1028, 2003.

[11] H. Pyo, O. Kwon, J. Seo, and E. Woo, "Identication of current density distribution in electrically conducting subject with anisotropic conductivity distribution," *Physics in Medicine and Biology*, vol. 50, no. 13, p. 3183-3196, 2005.

[12] C. Park, B. Lee, and O. Kwon, "Analysis of recoverable current from one component of magnetic flux density in MREIT and MRCDI," *Physics in medicine and biology*, vol. 52, no. 11, p. 3001-3013, 2007.

[13] T. DeMonte, R. Yoon, K. Hasanov, D. Jorgenson, and M. Joy, "Image distortion and image mis-registration in low frequency current density imaging," in *Engineering in Medicine and Biology, 2002. 24th Annual Conference and the Annual Fall Meeting of the Biomedical Engineering Society EMBS/BMES Conference, 2002. Proceedings of the Second Joint*, vol. 2. IEEE, 2002, pp. 933-934.

[14] T. DeMonte, R. Yoon, D. Jorgenson, and M. Joy, "Effects of gradient distortion on low frequency current density imaging," *ISMRM, XIth Sci. Meet. and Exh., Toronto, Canada*, 2003.

[15] P. Kostelec and S. Periaswamy, "Image registration for MRI," *Modern Signal Processing*, vol. 46, pp. 161-184, 2003.

[16] A. Gaudreau-Balderrama, "Multi-modal image registration," ISS Research Group, Department of Elec. & Comp Eng., Boston Univ., Tech. Rep., 2012.